XMM-*NEWTON* OBSERVATION OF θ^1 TAU, THE BRIGHTEST HYADES GIANT

R. Pallavicini[1], E. Franciosini[1], A. Maggio[1], G. Micela[1], M. Audard[2], and M. Güdel[2]

[1]INAF - Osservatorio Astronomico di Palermo, Piazza del Parlamento 1, I-90134 Palermo, Italy
[2]Paul Scherrer Institut, Laboratory for Astrophysics, 5232 Villingen, Switzerland

Abstract

We present an XMM-*Newton* observation of θ^1 Tau, the X-ray brightest giant in the Hyades open cluster. Spectral analysis using both the RGS and the EPIC instruments is presented and discussed. We have derived X-ray luminosities for the other three Hyades members falling in the XMM-*Newton* field of view; a comparison of the X-ray emission of the four Hyades stars with previous X-ray observations shows variations of less than a factor of 2 over two decades. We also report the detection of a flare from the field M dwarf star VA 479.

Key words: stars: coronae – stars: late-type – stars: abundances – stars: activity – stars: individual: θ^1 Tau

1. Introduction

θ^1 Tau (= VB 71 = HD 28307; spectral type K0 III) is one of the four giants in the Hyades open cluster, located at a distance of 48.4 pc (from Hipparcos, ESA 1997). This star has been previously observed in X-rays with *Einstein* (Stern et al. 1981; Micela et al. 1988), with *ROSAT*, during the All-Sky Survey (Stern et al. 1995) and in pointed PSPC observations (Pizzolato et al. 2000), and with *ASCA* (Ueda et al. 2001). Among the Hyades giants θ^1 Tau is the one with the highest X-ray emission level ($L_X \sim 10^{30}$ erg sec^{-1}), about a factor 50 more than ϵ Tau (the giant with the lowest X-ray luminosity).

The four Hyades giants are interesting for several reasons. They share the same position in the HR diagram and have very similar effective temperatures, gravities, masses, metallicities and rotational velocities. Yet, in spite of their very similar parameters, they show large differences in their chromospheric and coronal properties (Collura et al. 1993, Baliunas et al. 1998). These differences are unexplained in the context of our current understanding of dynamo activity and magnetic heating of stellar outer atmospheres. In addition, they are all "clump giants" in the helium burning phase and thus their chromospherc and coronal activity is expected to have strongly decreased after evolution along the red giant branch. X-ray emission is in fact extremely weak or absent in the most evolved giants (Schröder et al. 1998) and chromospheric Ca II emission decreases monotonically along the red giant branch (Dupree et al. 1999). Instead, the "clump giants" of the Hyades display substantial magnetic activity that has either survived or has been regenerated after the red giant phase. The origin of the high level of activity of the Hyades giants, and in particular of the brightest among them, remaints totally unexplained.

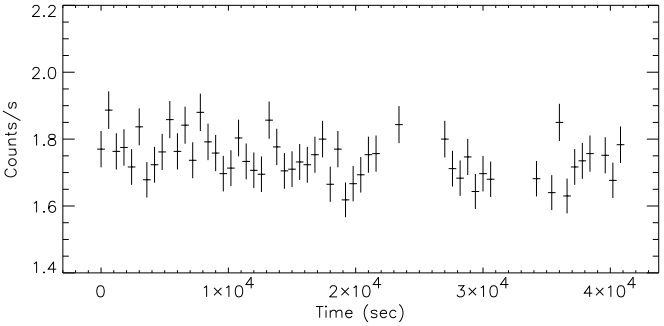

Figure 1. EPIC PN light curve of θ^1 Tau. Data are binned over 600 sec

In this paper we report on new X-ray observations of θ^1 Tau performed with the RGS and EPIC instruments aboard XMM-*Newton*. The second brightest giant (γ Tau) has been observed in another, yet unpublished, proprietary XMM-*Newton* observation (PI: N. Brickhouse).

2. Observations and data analysis

θ^1 Tau was observed by XMM-*Newton* on September 2–3, 2000, in two consecutive runs lasting 20 ksec and 48 ksec, respectively (IDs 0101440901 and 0101440501). For the first run no EPIC data are available (CAL CLOSED operation mode) and the RGS data are affected by a high background rate; we therefore present results obtained from the second run only. The EPIC camera was operated in the FullFrame mode using the thick filter for both MOS and PN. Effective exposure times are 48 ksec for RGS, 45 ksec for MOS and 42.5 ksec for PN.

Data analysis was performed using SAS v.5.2. Source light curves and spectra have been extracted from MOS and PN event files using an extraction region of 1′ radius, while background spectra were extracted from a concentric annulus with radii of 1.1′ and 1.7′ (the outer radius being limited by the presence of nearby sources). For the analysis of EPIC spectra, the standard response matrices released in December 2001 have been used. The spectra

Proc. Symposium *'New Visions of the X-ray Universe in the XMM-Newton and Chandra Era'* 26–30 November 2001, ESTEC, The Netherlands
ESA SP-488, August 2002 eds. F. Jansen & TBD

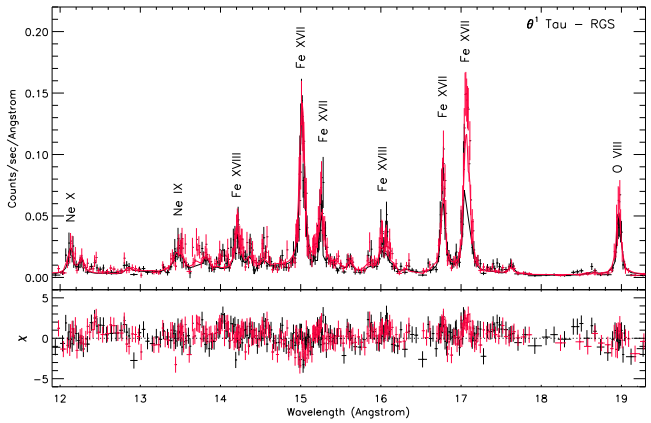

Figure 2. RGS1 (black) and RGS2 (red) spectrum of θ^1 Tau in the 12–19 Å wavelenght range. The best-fit 2-T model is also shown

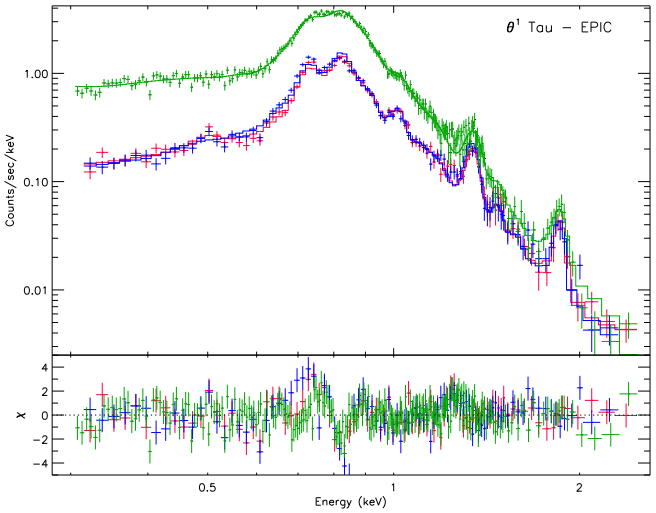

Figure 3. EPIC MOS1 (blue), MOS2 (red) and PN (green) spectra of θ^1 Tau. The individual best-fit 2-T models are also shown

have been binned in order to have at least 10 counts per energy bin for RGS, and 30 counts per bin for MOS and PN.

The PN light curve of θ^1 Tau is shown in Fig. 1: the source is steady, showing only low-level variability around a mean count rate of ~ 1.7 counts/sec in the PN instrument, and ~ 0.5 counts/sec in each MOS instrument.

3. Spectral analysis

We have performed a joint fit of RGS1, RGS2 and MOS1 spectra, and separate fits of MOS1, MOS2 and PN spectra, using two-temperature thermal models, adopting the APEC v.1.10 emissivities available in XSPEC v.11.1.0. The abundances of C, N, O, Ne, Mg, Si, S, Fe, and Ni were treated as individual free parameters, while the other abundances were fixed at solar values. The interstellar hydrogen column density was left free to vary but in all cases it converged to a negligible value. The individual EPIC spectra have been fitted in the 0.3–2.5 keV range. Because of the inaccuracy and incompleteness of atomic data for non-Fe L-shell transitions, significant parts of the RGS spectra had to be discarded above 20 Å; furthermore, some Fe L-shell lines with inaccurate atomic data were not fitted. Also, in the joint RGS+MOS1 fit the MOS1 data with $\lambda \geq 9.65$ Å were discarded to favor the use of the high-resolution RGS data. For additional information on the RGS data analysis, we refer to Audard et al. (2002) and Güdel et al. (2002).

Table 1. Best-fit parameters of the 2-T APEC model. Errors are 90% confidence ranges computed for one interesting parameter

	RGS+MOS1	MOS1	MOS2	PN
kT_1^a	$0.31^{+0.03}_{-0.03}$	$0.38^{+0.05}_{-0.04}$	$0.35^{+0.03}_{-0.02}$	$0.26^{+0.01}_{-0.02}$
kT_2^a	$0.56^{+0.02}_{-0.01}$	$0.62^{+0.07}_{-0.04}$	$0.60^{+0.03}_{-0.02}$	$0.57^{+0.01}_{-0.02}$
EM_1^b	$3.84^{+1.77}_{-0.98}$	$4.46^{+0.76}_{-1.74}$	$4.49^{+0.53}_{-1.18}$	$3.08^{+0.64}_{-1.04}$
EM_2^b	$3.70^{+1.46}_{-0.67}$	$1.91^{+0.53}_{-0.64}$	$1.77^{+0.31}_{-0.42}$	$2.38^{+0.45}_{-0.53}$
C	$0.18^{+0.14}_{-0.14}$	$0.20^{+1.39}_{-0.20}$	$1.04^{+0.89}_{-1.04}$	$0.00^{+0.31}_{-0.00}$
N	$0.38^{+0.21}_{-0.16}$	$0.75^{+0.64}_{-0.75}$	$0.00^{+0.32}_{-0.00}$	$0.62^{+0.69}_{-0.33}$
O	$0.14^{+0.05}_{-0.04}$	$0.13^{+0.04}_{-0.05}$	$0.20^{+0.04}_{-0.05}$	$0.20^{+0.10}_{-0.04}$
Ne	$0.22^{+0.07}_{-0.06}$	$0.35^{+0.09}_{-0.10}$	$0.38^{+0.09}_{-0.10}$	$0.81^{+0.23}_{-0.21}$
Mg	$0.73^{+0.20}_{-0.24}$	$0.97^{+0.21}_{-0.23}$	$1.26^{+0.23}_{-0.11}$	$1.29^{+0.45}_{-0.24}$
Si	$0.74^{+0.23}_{-0.29}$	$0.84^{+0.32}_{-0.18}$	$1.08^{+0.34}_{-0.21}$	$0.76^{+0.14}_{-0.17}$
S	$0.84^{+0.72}_{-0.54}$	$1.03^{+0.70}_{-0.66}$	$0.00^{+1.37}_{-0.00}$	$0.00^{+0.23}_{-0.00}$
Fe	$0.60^{+0.13}_{-0.16}$	$0.75^{+0.08}_{-0.14}$	$0.89^{+0.11}_{-0.13}$	$1.15^{+0.41}_{-0.15}$
Ni	$0.00^{+0.08}_{-0.00}$	$0.00^{+0.22}_{-0.00}$	$0.00^{+0.17}_{-0.00}$	$0.00^{+0.79}_{-0.00}$
χ^2_r	1.17	1.60	2.45	1.09
d.o.f.	450	81	82	241

[a] kT in keV
[b] EM in units of 10^{52} cm^{-3}

The best-fit parameters are given in Table 1. Fig. 2 shows the RGS1 and RGS2 spectra and the joint best-fit model in the 12–19 Å wavelength range. The X-ray spectrum of θ^1 Tau is largely dominated by the bright Fe XVII and Fe XVIII L-shell lines, indicating a dominant temperature component around 0.6 keV, confirmed by our analysis (Table 1). However, other transitions are observed, e.g. Lyα transitions from O VIII, Ne X, N VII, and C VI.

Fig. 3 shows the three EPIC spectra with the individual best-fit models. The EPIC MOS fits are not acceptable, from a statistical point of view ($\chi^2_r = 1.6$ for 81 d.o.f. for MOS1, and $\chi^2_r = 2.4$ for 82 d.o.f. for MOS2), due to large residuals in the ranges 0.6–0.9 keV and 1.1–1.3 keV. Adding a third plasma component does not improve the fit: indeed, any additional component always converges to one of the first two. The large residuals may arise from inadequacies of the currently available plasma codes or from calibration problems. For example, the discrepancy around 1.2 keV is possibly due to the existence of additional lines, due to transitions from high-n states in

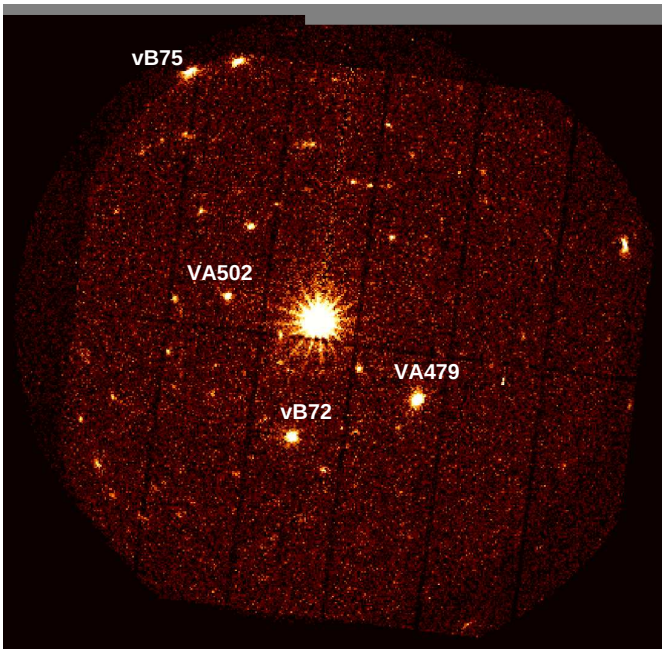

Figure 4. Composite EPIC MOS1+MOS2+PN image of the observed field of view. The brightest source in the center is θ^1 Tau. Labels indicate the other identified sources

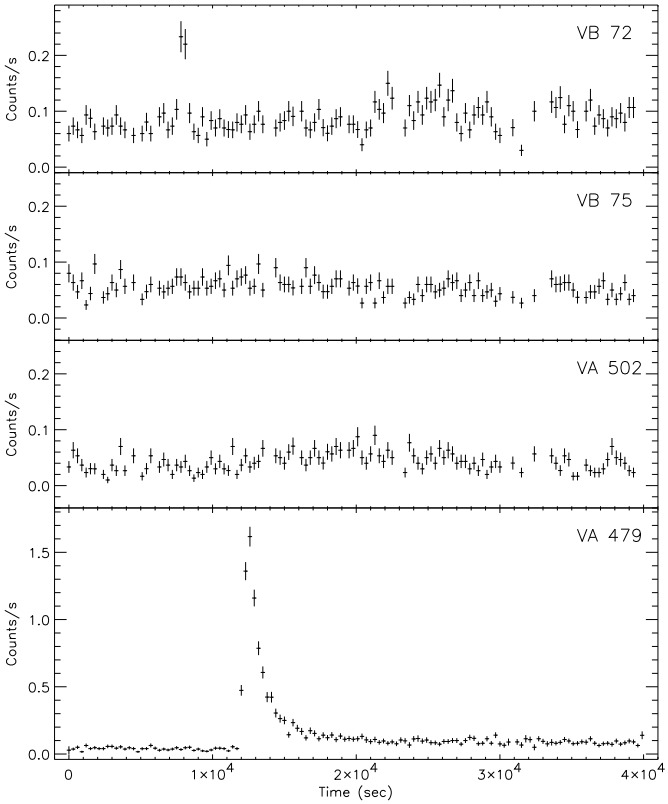

Figure 5. X-ray light curves of the other identified sources in the field of view. Data are binned over 300 sec

Fe XVII–XIX ions (Brickhouse et al. 2000), not yet included in the plasma emission models available in XSPEC.

We also note that, while in general the best-fit parameters derived from different instruments agree within the errors, some discrepancies are still present, that are likely due to uncertainties in the cross-calibration of the instruments.

4. Other sources in the field of view

Fig. 4 shows the combined MOS1+MOS2+PN image of the XMM-*Newton* field of view: besides θ^1 Tau, several other sources are evident. A preliminary source detection performed on the combined dataset using the Maximum Likelihood (ML) algorithm resulted in the detection of $\sim$ 140 sources with $ML > 10$ (4σ). In addition to θ^1 Tau, we have clearly detected all the other three known Hyades members that fall in the XMM-*Newton* field of view, i.e. VB 72 (= θ^2 Tau = HD 28319, spectral type A7III, SB1), VB 75 (= HD 28363, spectral type F7V+G0V) and VA 502 (spectral type K7Ve). The latter star has been detected for the first time, with an X-ray luminosity of 9×10^{27} erg sec^{-1}, which is a factor of 2–3 lower than the sensitivity limit of the previous X-ray surveys of the Hyades cluster (Micela et al. 1988; Stern et al. 1995). X-ray light curves of these stars are shown in the upper three panels of Fig. 5. The sources have a nearly constant emission level, except for a flare occurring on VB 72 about 2 hours after the start of the observation, with a duration of $\sim$ 1000 sec, and an increase in the count rate by a factor of $\sim$ 3.

A much stronger flare has been detected from another source in the field of view (lowest panel of Fig. 5): the count rate increased by a factor of $\sim$ 30 in less than 1000 sec, and decayed with an e-folding time of $\sim$ 1400 sec. We have identified the source with VA 479, an M-type star which has been rejected as a Hyades member on the basis of its proper motion, and is probably a background field star.

4.1. Long-term variability of Hyades members

θ^1 Tau, VB 72 and VB 75 had all been detected in the previous *Einstein*, *ROSAT* and *ASCA* observations; this allows us to investigate the long-term variability of the X-ray emission. We have computed X-ray luminosities in the 0.1-2.4 keV range, using a conversion factor of 7.1×10^{-12} erg cm^{-2} per MOS count, derived from the best-fit model for θ^1 Tau, and using individual distances from Hipparcos. The *ASCA* luminosities were derived similarly from the count rates reported in the *ASCA* Medium Sensitivity Survey Catalogue (Ueda et al. 2001), while *Einstein* and *ROSAT* luminosities were taken from Micela et al. 1988 and Stern et al. 1995, and corrected for the new distances. The comparison between the XMM-*Newton* and previous luminosities is shown in Fig. 6: the emission levels are very similar, with variations of at most a factor of $\sim$ 2 over $\sim$ 20 years. The only exception is VB 72 which was a factor of

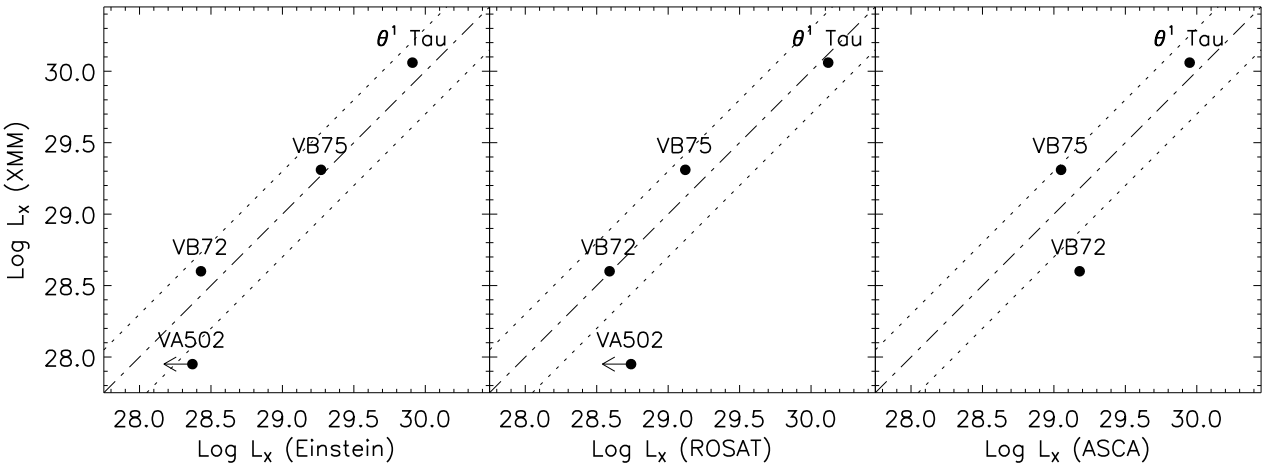

Figure 6. Comparison of the X-ray luminosities of the Hyades members measured by XMM-Newton with those derived from Einstein, ROSAT and ASCA. Luminosities have been recomputed using the individual Hipparcos distances. The dot-dashed line represent equal luminosities; the dotted lines indicate variations of a factor of 2

$\sim 4-5$ brighter during the *ASCA* observation: given the similar emission levels observed at other times, it is likely that the star was undergoing a flaring event.

5. Conclusions

Our observation of θ^1 Tau with XMM-*Newton* has confirmed the strong coronal emission of this helium-burning clump giant, at a level comparable to that of previous observations by *Einstein*, *ROSAT* and *ASCA*. The EPIC and RGS spectra have allowed us to model the source with a 2-T thermal model with $T_1 \sim 3.5\times10^6$ K and $T_2 \sim 6.7\times10^6$ K and an emission measure $EM \sim 2-4\times10^{52}$ cm^{-3} for both components. The derived coronal abundances for C, N, O, Ne, Mg, Si, S, Fe and Ni are solar or subsolar, within the errors, with some evidence for a FIP effect: low-FIP elements, such as Mg, Fe and Si, have higher abundances than the high-FIP elements O and Ne. However, some discrepancies exist between the abundances derived from different instruments which point at possible uncertainties in their cross-calibration. The large residuals present at specific wavelengths in some of the fits also suggest the existence of either calibration problems or inadequacies in the currently available plasma codes. For this reason the results of the spectral fits should be considered preliminary at this stage. The low S/N of the RGS spectrum at the O VII triplet prevents a determination of the plasma electron density from the ratio of the intercombination and forbidden lines.

The XMM-*Newton* observation of this Hyades field reveals the presence of ~ 140 X-ray sources of which only 4 belong to the Hyades. Comparison of these Hyades sources with previous observations by *Einstein*, *ROSAT* and *ASCA* show for all of them (except for VA 502 previously undetected) variations of less than a factor 2; in particular, θ^1 Tau appears remarkably constant over a time period of 20 years. A small flare has been detected by XMM-*Newton* from the Hyades star VB 72, while a much stronger flare has been detected from the M dwarf VA 479 not belonging to the Hyades cluster. It will be interesting to compare our results for θ^1 Tau with the XMM-*Newton* observation of γ Tau, the second brightest Hyades giant, as soon as the latter observation will become public.

References

Audard, M., Güdel, M., et al. 2002, A&A, in preparation
Baliunas, S.L., Donahue, R.A., Soon, W., & Henry, G.W. 1998, in: ASP Conf. Ser. 154, Tenth Cool Stars, Stellar Systems and the Sun, eds. R.A. Donahue & J. Bookbinder, 153
Brickhouse, N.S., Dupree, A.K., Edgar, R.J., et al. 2000, ApJ 530, 387
Collura, A., Maggio, A., Micela, G., et al. 1993, ApJ 416, 204
Dupree, A.K., Whitney, B.A., & Pasquini, L. 1999, ApJ 520, 751
Güdel, M., Audard, M., Sres, A., Wehrli, R., & Mewe, R. 2002, ApJ, submitted
Micela, G., Sciortino, S., Vaiana, G.S., et al. 1988, ApJ 325, 798
Schröder, K.-P., Hünsch, M., & Schmitt, J.H.M.M. 1998, A&A 335, 591
Stern, R.A., Zolcinski, M.-C., Antiochos, S.K., & Underwood, J.H. 1981, ApJ 249, 647
Stern, R.A., Schmitt, J.H.M.M., & Kahabka, P.T. 1995, ApJ 448, 683
Pizzolato N., Maggio A., & Sciortino S. 2000, A&A 361, 614
Ueda, Y., Ishisaki, Y., Takahashi, T., Makishima, K., & Ohashi, T. 2001, ApJS 133, 1